07

Efficiency of concentrator photovoltaic modules based on short-focus Fresnel lenses and A^3B^5 solar cells

© V.M. Emelyanov, S.A. Levina, M.V. Nakhimovich, A.A. Soluyanov, M.Z. Shvarts

Ioffe Institute,
194021 St. Petersburg, Russia
e-mail: vm.emelyanov@mail.ioffe.ru

Received April 14, 2024
Revised July 1, 2024
Accepted July 2, 2024

The efficiency of concentrator photovoltaic modules built on the basis of highly efficient cascade GaInP/GaAs/Ge solar cells and 60×60 mm Fresnel lenses of the („silicon on glass“) type with a shortened focal length has been studied. A simulation of the spatial distributions of photocurrents for subelements of a cascade solar cell was carried out, on the basis of which the current-voltage characteristics and the dependence of the efficiency on the focal length of Fresnel lenses in the range of 85–125 mm. Also the permissible misorientation angle of the photovoltaic module from the direction to the Sun were calculated. It was found that reducing the focal length from 125 mm, which is optimal in terms of efficiency for a lens of the selected size, to 105 mm leads to a decrease in efficiency by no more than 0.3 abs% at misorientation angles up to 2°. The consequence of further reduction of the focal length of the lens to 85 mm is a decrease in the efficiency of the module by 0.6–1.2 abs.%.

Keywords: Fresnel lens, multijunction solar cell, concentrator photovoltaic module, efficiency, misorientation angle.

DOI: 10.61011/TP.2024.10.59363.133-24

Introduction

The construction of solar photovoltaic arrays (SPVAs) based on modules with optical concentrators of solar radiation is one of the most promising methods for reducing the cost of energy generated by a solar power plant. Their efficiency may be maximized by using cascade (multijunction) solar cells (SCs) based on A^3B^5 heterostructures with an efficiency higher than 40% under terrestrial conditions (solar spectrum AM1.5D) and optical concentrators („silicon on glass“ Fresnel lenses (FLs)) [1–8]. Such FLs are rather cheap to produce and provide an opportunity both to reduce the cost of a concentrator photovoltaic module (CPVM) through more efficient use of expensive A^3B^5 heterostructures and to improve the thermodynamic conditions of conversion of solar radiation in SCs.

An efficiency in excess of 36% [5,6] was demonstrated for FLATCON CPVMs with four-junction A_3B_5 solar cells. The efficiency of CPVMs based on series-produced three-junction GaInP/Ga(In)As/Ge SCs is 34% or more [4,7].

It should be noted that the cost of FLs and SCs in CPVMs is not the only parameter that determines the cost of electricity produced by SPVAs. It is also affected by

— overall material consumption;

— costs associated with production and maintenance of the pointing system, which increase as the requirements for pointing accuracy become more stringent.

At the same time, relaxed requirements as to the pointing accuracy necessitate the use of a larger SC area to absorb solar radiation under the conditions of focal point displacement relative to the FL optical axis, and this, in turn, leads both to an increase in the cost of a square meter of the CPVM area (due to an increase in the A^3B^5 heterostructure area) and to a reduction in the SC efficiency due to an increase (proportional to the $p-n$ junction area) in the densities of injection and recombination currents and ohmic losses in longer contact bars.

It was demonstrated in [9] that an FL made of a given material has a unique combination of design parameters (size (aperture), focal length, and profile pitch) minimizing the size of a spot into which collected radiation is focused. Since the profile pitch is a technological parameter, it is fair to say that a certain optimum focal length, which ensures minimization of the spot of concentrated radiation on the SC surface, corresponds to a given FL size and a given tooth pitch. The design solutions for SMALFOC CPVMs with a reduced height discussed in [10] ensure reduction of the design focal length of the FL from 125 mm (the optimum lens with a minimum radius of the focal light spot) to 85 mm without any significant loss of optical efficiency. However, short-focus FLs have two distinctive features:

(1) with a slight increase in the focal point size, the light power density in the center of a short-focus (85 mm) FL increases by a factor up to 1.5 (in comparison with the same parameter for the optimum lens), which leads to an increase in ohmic losses and a reduction in SC efficiency;

(2) the magnitude of shift of the radiation maximum in the focal plane due to misorientation is proportional to the focal length, which allows one to modify CPVMs with a shortened focal length by either reducing the SC size

to improve their efficiency or increasing the permissible misorientation angle (error of solar pointing).

Thus, a study of the dependence of efficiency of CPVMs with a reduced design height on their key parameters (FL focal length and permissible angle of CPVM misorientation relative to the direction to the Sun) is relevant to the assessment of feasibility of construction of SPVAs based on such modules. The results of simulation of the photovoltaic characteristics of CPVMs based on „silicon on glass" FLs 60×60 mm in size and commercially available three-junction high-efficiency GaInP/GaAs/Ge SCs are reported below. In what follows, both a separate concentrator „FL–SC" cell and an array of such cells combined into a module are denoted as a CPVM. Electrical connection losses are not discussed.

1. Simulation of photovoltaic characteristics of CPVMs

The photovoltaic characteristics of CPVMs were calculated in the case of irradiation with direct sunlight of the terrestrial spectrum under standard conditions (AM1.5D, 1000 W/m^2, 25°C). This problem was solved in several stages:

(1) shaping the profile of an FL with an aperture of 60×60 mm and a given focal length in accordance with the procedure outlined in [11,12] and finding the spectral optical-energy characteristics (distributions of irradiance in the focal plane for different wavelengths) for it;

(2) calculating the spatial distributions of photocurrent densities for SC subcells based on the irradiance distributions and spectral dependences of the external quantum yield of the photoresponse;

(3) simulation of I-V characteristics of solar cells based on the spatial distributions of photocurrents.

Modeling of the spectral optical-energy FL characteristics and profiling of photocurrent generation in subcells of a multijunction SC were performed using a ray tracing tool (model) [11,12]. The radiation flux passing through the lens was simulated by a large number of cones of rays. Each beam from a cone was normalized in energy and traced to its intersection with the SC surface, where the energy contributions of beams in the cells of the formed radial-ring grid were summed up. The photocurrent density was calculated for each cell:

$$J_{ph,m}(i) = \frac{e}{hc} \sum_{k=1}^{N} \sigma_i \Phi_i^{\lambda_{k-1} \cdots \lambda_k} \times \int_{\lambda_{k-1}}^{\lambda_k} \lambda \Gamma(\lambda) Q_{em}(\lambda) d\lambda \cdot \left[\int_{\lambda_{k-1}}^{\lambda_k} \Gamma(\lambda) d\lambda \right]^{-1}, \quad (1)$$

where i is the cell index, σ_i is the cell area, $\Phi_i^{\lambda_{k-1} \cdots \lambda_k}$ is the optical power density within spectral range $[\lambda_{k-1}, \lambda_k]$, $Q_{em}(\lambda)$ is the external quantum yield of subcell m, $\Gamma(\lambda)$ is the spectral density of irradiance of beam (direct) radiation, λ is the wavelength, e is the elementary charge, h is the Planck constant, c is the speed of light in vacuum, and N is the number of ranges into which the radiation spectrum is divided. The integrals with spectral density of irradiance were introduced to compensate for errors associated with the choice of step for $\Phi_i^{\lambda_{k-1} \cdots \lambda_k}$ spectral ranges, which normally vary from 50 to 100 nm.

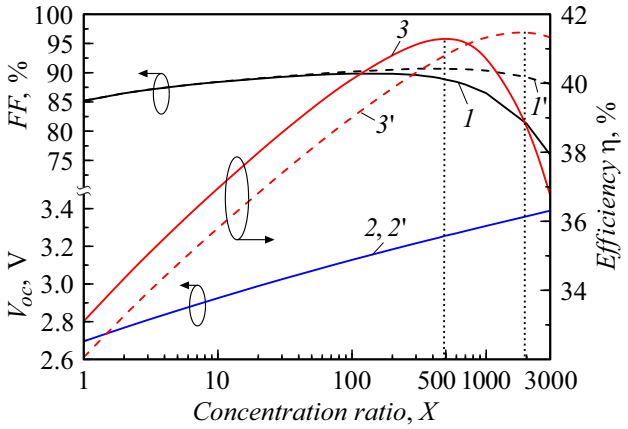

Figure 1. Dependences of photovoltaic parameters of the GaInP/GaAs/Ge SC, which was used as a prototype, on the solar radiation concentration ratio (AM1.5D spectrum) with uniform distribution of the receiver surface irradiance: *1, 1'* — fill factor *FF*; *2, 2'* — open-circuit voltage V_{oc} (the plots merge in the scale of the figure); *3, 3'* — efficiency η. Solid curves (*1–3*) correspond to a contact grid pitch of 100 μm, while dashed curves (*1'–3'*) correspond to a pitch of 50 μm.

The photovoltaic characteristics were simulated for a three-junction GaInP/GaAs/Ge SC. Its I-V characteristics were calculated using a three-dimensional distributed equivalent circuit [13]. The primary contribution to the series SC resistance was produced by the resistance to current flow under the contact grid in the lateral direction and the resistance of contact bars. Their characteristic values were taken into account in accordance with the approach proposed in [14]

The characteristic resistance to lateral current flow was calculated in the following way:

$$R_{sheet} = \frac{R_L}{4} \left(\frac{s}{A} \right)^2, \qquad R_L = \left(\frac{d_{win}}{\rho_{win}} + \frac{d_{top}}{\rho_{top}} \right)^{-1}, \quad (2)$$

where R_L is the sheet resistance under the contact grid (resistance to lateral current of a section with its width and length equal to 1 cm), ρ_{win}, ρ_{top} are the specific resistances of the wide-bandgap „window" and the front layer (emitter) of the top subcell of the cascade SC, d_{win}, d_{top} are their thicknesses, s is the contact grid pitch, and A is the linear size (side length) of the SC.

Parameters of GaInP/GaAs/Ge SCs used in I-V characteristics simulation

Parameter	Value		
Photocurrent density for subcells (AM1.5D, 1000 W/cm^2), mA/cm^2	GaInP	GaAs	Ge
	15.87	15.03	19.23
Density of the injection (diffusion) $p-n$ junction current, A/cm^2	$3.0 \cdot 10^{-27}$	$4.9 \cdot 10^{-21}$	$3.4 \cdot 10^{-6}$
Density of the recombination $p-n$ junction current, A/cm^2	$3.1 \cdot 10^{-14}$	$2.2 \cdot 10^{-12}$	–
Sheet resistance under the contact grid, Ω/□	1190		
Specific resistance of the contact grid material (gold), Ω·cm	$2.35 \cdot 10^{-6}$		
Contact grid pitch, μm	100	50	
Contact bar width, μm	5	4	
Contact bar thickness, μm	5	4	

The characteristic resistance of the contact grid with a two-dimensional pattern was given by

$$R_{grid} = \frac{1}{8}\frac{\rho_{grid}}{d_{grid}}\frac{s}{w}, \qquad (3)$$

where ρ_{grid} is the specific resistance of the grid material and d_{grid}, w are the thickness and the width of fingers.

The SC parameters used in modeling were calculated based on the experimental spectral dependences of the external quantum yield of photoresponse for subcells and the I-V characteristic of the SC prototype (see the table). The photovoltaic SC characteristics under uniform illumination for two values of the contact grid pitch are shown in Fig. 1. The maximum efficiency of the studied three-junction GaInP/GaAs/Ge SC exceeded 41%.

2. Effect of design parameters of CPVMs on their characteristics

The photocurrent generation profiles of subcells were calculated for the chosen GaInP/GaAs/Ge multijunction receiver prototype positioned in the focal plane of a radiation concentrator in order to examine the dependence of CPVM efficiency on the FL and SC design parameters. The magnitude of ohmic losses due to the flow of lateral currents in layers below the contact grid depends significantly on the local photocurrent density in the top subcell of the cascade SC. The photocurrent distributions corresponding to the top GaInP subcell calculated for the optimum lens ($F = 125$ mm, [9,10]) and for short-focus FLs are shown in Fig. 2.

The distributions presented in Fig. 2 illustrate well the differences in the SC operating conditions under FLs with different focal lengths: the maximum photocurrent density increases significantly with a reduction in focal length (this is true for all subcells). However, unlike the middle GaAs and bottom Ge subcells, the top GaInP subcell has its photocurrent collected by the contact grid for transmission to the external circuit (in the case of GaAs and Ge subcells, heavily doped layers of tunnel diodes act as connection elements). This translates into dominance of the lateral component of current flow in the thin GaInP $p-n$ junction emitter layers and the wide-bandgap window and, consequently, into an increased contribution of the sheet resistance under the contact grid to the series SC resistance.

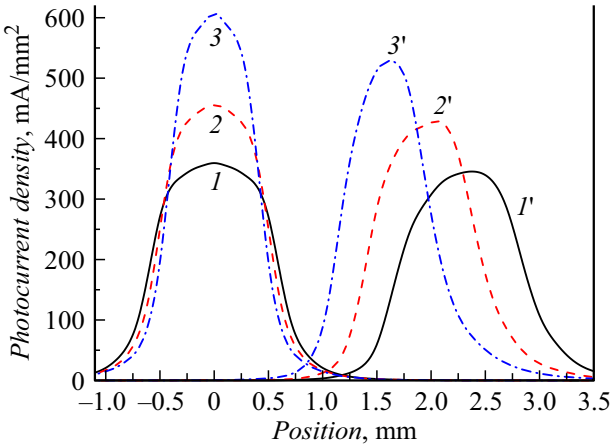

Figure 2. Distributions of photocurrent in the GaInP subcell of the GaInP/GaAs/Ge SC operating with an FL under normal incidence of sunlight (AM1.5D, 1000 W/m^2) onto the CPVM (*1–3*) and with angle $\alpha = 1^\circ$ of CPVM misorientation with respect to the direction to the Sun (*1'–3'*) for different FL focal lengths: *1, 1'* — 125; *2, 2'* — 105; *3, 3'* — 85 mm.

In the case of misorientation, the magnitude of longitudinal (along the SC surface) displacement of the maximum of the local photocurrent density is inversely proportional to the FL focal length (Fig. 2). This is illustrated in more detail in Fig. 3: as the misorientation angle increases, the max-

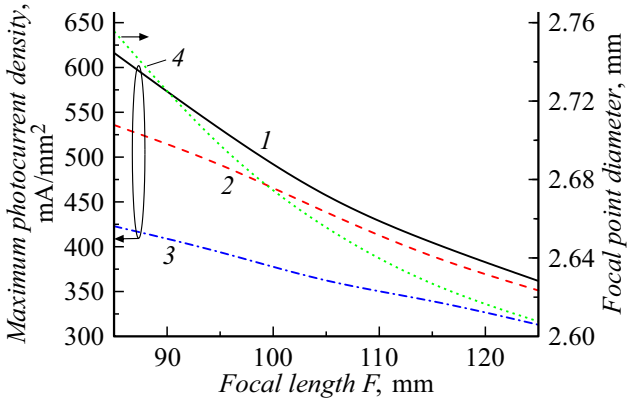

Figure 3. Dependences of the maximum local photocurrent density (*1–3*) of the GaInP subcell of the GaInP/GaAs/Ge SC in a CPVM and the focal point diameter (*4*) on the FL focal length. *1, 4* — Normal incidence of radiation onto the CPVM; *2, 3* — angles $\alpha = 1$ and 2° of CPVM misorientation with respect to the direction to the Sun, respectively. CPVM irradiation conditions: AM1.5D, 1000 W/m^2.

imum (peak) photocurrent density decreases significantly (Fig. 3, curves *1–3*). The SC area within which 95% of the photocurrent of each of the three subcells is generated depends only on the focal length (Fig. 3, curve *4*).

3. Results and discussion

The simulated photocurrent distributions for square SCs with a side length varying from 2.6 to 12 mm and parameters indicated the table were used to estimate the CPVM efficiency as a function of the design FL focal length and permissible angle α_{max} of module misorientation with respect to the direction to the Sun (the angle within which 95% of the optical power is concentrated on the SC surface).

The influence of the contact grid pitch on efficiency is illustrated in Fig. 4. It is evident that a pitch of 100 μm is insufficient for FLs with focal lengths $F = 125$ mm and $F = 85$ mm. Notably, the efficiency of the CPVM with a short-focus lens is lower for all the examined SC sizes. Thus, the SC design with a contact grid pitch of 50 μm is suggested for further evaluation.

It should also be noted that the efficiency decreases with increasing SC size due to the growth of the $p-n$ junction area and the operating voltage reduction. The dependence of the permissible misorientation angle on SC size turns out to be almost linear. A focal length reduction from 125 to 85 mm allows one to increase the permissible angle of misorientation by 15% only, which is attributable to the slight increase in diameter of the focal point formed by the short-focus lens (Fig. 3, curve *4*).

Figure 5 presents the dependences of CPVM efficiency on the permissible misorientation angle for five different FL focal lengths. Compared to a lens with focal length $F = 125$ mm, a lens with $F = 115$ mm provides a CPVM efficiency only 0.25 abs.% lower at misorientation angles up to 0.5°. At angles greater than 1.2°, the predicted efficiency levels of modules based on FLs with $F = 115$ and 125 mm are virtually identical. Compared to the module based on the optimum FL ($F = 125$ mm), CPVMs with short-focus FLs ($F = 95$ and 85 mm) have 0.8–0.3 abs.% and 1.35–0.5 abs.% lower predicted efficiencies, respectively, corresponding to misorientation angles increasing up to 2°.

The dependences of CPVM efficiency and SC side length needed to intercept (receive) 95% of the luminous flux concentrated by the lens on the FL focal length are shown in Fig. 6. The plots for three values of the permissible misorientation angle are presented. The SC side length sufficient for radiation reception increases slightly with focal

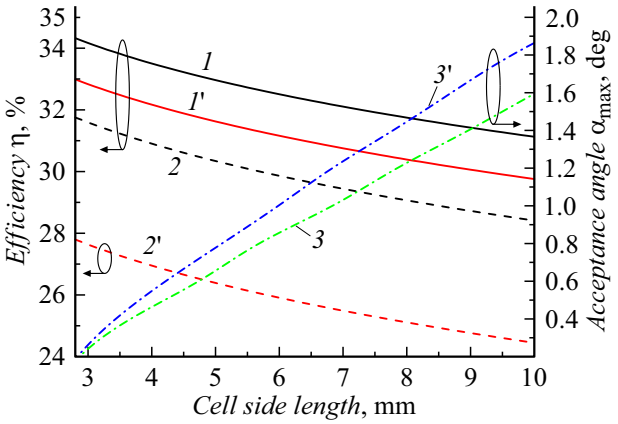

Figure 4. Dependences of the efficiency and permissible misorientation angle σ_{max} of the CPVM based on GaInP/GaAs/Ge SCs and FLs with focal length $F = 125$ mm (*1–3*) and $F = 85$ mm (*1'–3'*) on the SC side length: *1, 1'* — efficiency of the SC with a contact grid pitch of 50 μm; *2,2'* — efficiency of the SC with a contact grid pitch of 100 μm; *3, 3'* — permissible misorientation angle with the SC receiving 95% of the luminous flux concentrated by the lens. CPVM irradiation conditions: AM1.5D, 1000 W/m^2.

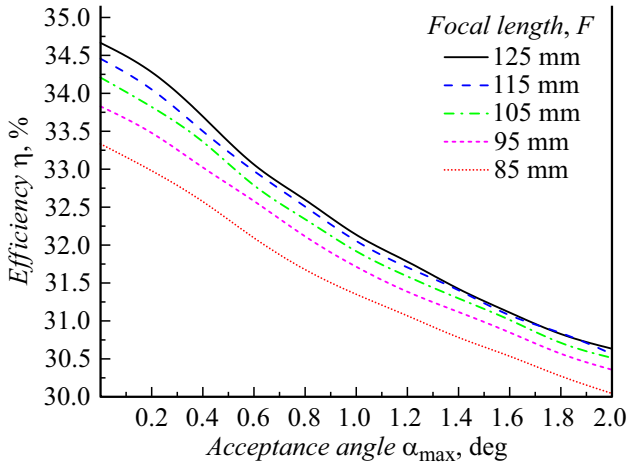

Figure 5. Model dependences of the efficiency of the CPVM based on GaInP/GaAs/Ge SCs and FLs with different focal lengths F on the permissible misorientation angle. CPVM irradiation conditions: AM1.5D, 1000 W/m^2.

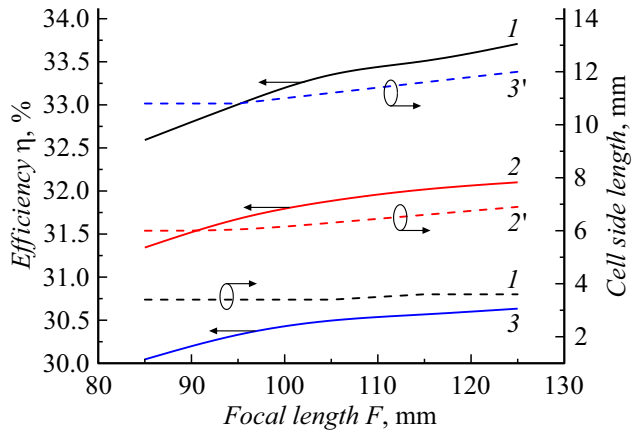

Figure 6. Efficiency of the CPVM based on GaInP/GaAs/Ge SCs (*1–3*) and required cell side length (*1'–3'*) as functions of the FL focal length for various permissible misorientation angles: *1, 1'* — $\sigma_{max} = 0.4°$, *2, 2'* — $\sigma_{max} = 1°$; *3, 3'* — $\sigma_{max} = 2°$. CPVM irradiation conditions: AM1.5D, 1000 W/m^2.

length: from 3.4 to 3.6 mm at permissible misorientation angle $\alpha_{max} = 0.4°$, from 6.0 to 6.9 mm at $\alpha_{max} = 1°$, and from 10.8 to 12.0 mm at $\alpha_{max} = 2°$.

As the focal length increases from 85 mm (short-focus FL) to 125 mm (optimum FL), the efficiency varies within the 32.6–33.7 abs.%, 31.4–32.1 abs.%, and 30.0–30.6 abs.% ranges at permissible misorientation angles (α_{max}) of 0.4°, 1°, and 2°, respectively. It should be noted that the dependence of efficiency on the FL focal length within the 85–105 mm range is more pronounced than in the 105–125 mm range.

Conclusion

The obtained results demonstrate that a 16% reduction in focal length (from 125 to 105 mm) of „silicon on glass“ FLs with an aperture of 60 × 60 mm leads to a 0.1–0.3 abs.% reduction in efficiency of CPVMs based on GaInP/GaAs/Ge SCs converting solar radiation of the terrestrial spectrum (AM1.5D, 1000 W/m^2) within the established range of permissible misorientation angles (up to $\alpha_{max} = 2°$). If the focal length is shortened further to 85 mm (by 32% relative to the optimum lens with $F = 125$ mm), an additional 0.6–1.2 abs.% reduction in CPVM efficiency is observed. The use of shorter-focus FLs provides no economically significant practical reduction in size of a solar cell and, consequently, its area. The corresponding parameters should be taken into account in the process of construction of SMALFOC CPVMs based on FLs with shorter focal lengths and A^3B^5 multijunction SCs.

.

Conflict of interest

The authors declare that they have no conflict of interest.

References

[1] M.A. Green, E.D. Dunlop, M. Yoshita, N. Kopidakis, K. Bothe, G. Siefer, X. Hao. Prog. in PV: Res. and Appl., **32** (1), 3 (2024). DOI: 10.1002/pip.3750

[2] C. Algora, I. Rey-Stolle (eds.). *Handbook on Concentrator Photovoltaic Technology* (John Wiley & Sons, NY., 2016), DOI: 10.1002/9781118755655

[3] M. Wiesenfarth, I. Anton, A.W. Bett. Appl. Phys. Rev., **5** (4), 041601 (2018). DOI: 10.1063/1.5046752

[4] M. Wiesenfarth, M. Steiner, T. Dörsam, G. Siefer, F. Dimroth, P. Nitz, A.W. Bett. AIP Conf. Proc., **2149**, 030007 (2019). DOI: 10.1063/1.5124184

[5] M. Steiner, A. Bösch, A. Dilger, F. Dimroth, T. Dörsam, M. Muller, T. Hornung, G. Siefer, M. Wiesenfarth, A.W. Bett. Prog. in PV: Res. Appl., **23** (10), 1323 (2015). DOI: 10.1002/pip.2568

[6] S. van Riesen, M. Neubauer, A. Boos, M.M. Rico, C. Gourdel, S. Wanka, R. Krause, P. Guernard, A. Gombert. AIP Conf. Proc., **1679**, 100006 (2015). DOI: 10.1063/1.4931553

[7] E.A. Ionova, N.Yu. Davidyuk, N.A. Sadchikov, A.V. Andreeva. Tech. Phys., **66** (9), 1208 (2021). DOI: 10.1134/S1063784221090073

[8] A.V. Chekalin, A.V. Andreeva, N.Yu. Davidyuk, N.S. Potapovich, N.A. Sadchikov, V.M. Andreev, D.A. Malevskii. Tech. Phys., **66** (6), 857 (2021). DOI: 10.1134/S1063784221060050

[9] M.Z. Shvarts, V.M. Emelyanov, M.V. Nakhimovich, A.A. Soluyanov, V.M. Andreev. AIP Conf. Proceed., **2149**, 070011 (2019). DOI: 10.1063/1.5124210

[10] M.Z. Shvarts, V.M. Emel'yanov, S.A. Levina, M.V. Nakhimovich, A.A. Soluyanov. Pis'ma Zh. Tekh. Fiz., **50** (18), 7 (2024) (in Russian). DOI: 10.61011/PJTF.2024.07.57461.19823

[11] M.Z. Shvarts, V.M. Andreev, V.S. Gorohov, V.A. Grilikhes, A.E. Petrenko, A.A. Soluyanov, N.H. Timoshina, E.V. Vlasova, E.M. Zaharevich. Proc. 33rd IEEE PVSC (2008), paper 403. DOI: 10.1109/PVSC.2008.4922751

[12] M.Z. Shvarts, A.A. Soluyanov. Adv. Sci. Technol., **74**, 188 (2010). DOI: 10.4028/www.scientific.net/AST.74.188

[13] V.M. Emelyanov, N.A. Kalyuznyy, M.A. Mintairov, S.A. Mintairov, M.Z. Shvarts, V.M. Lantratov. Proc. 25th EU PVSEC, 406 (2012). DOI: 10.4229/25thEUPVSEC2010-1DV.2.33

[14] V.M. Emelyanov, S.A. Mintairov, S.V. Sorokina, V.P. Khvostikov, M.Z. Shvarts. Semiconductors, **50** (1), 125 (2016). DOI: 10.1134/S1063782616010085

Translated by D.Safin